Available online at www.sciencedirect.com

ScienceDirect

Ceramics International 40 (2014) 2979–2984

CERAMICS INTERNATIONAL

www.elsevier.com/locate/ceramint

Enhancement of the dielectric, piezoelectric, and ferroelectric properties in $BiYbO_3$-modified $(Ba_{0.85}Ca_{0.15})(Ti_{0.9}Zr_{0.1})O_3$ lead-free ceramics

Jiafeng Ma[a,*], Xinyu Liu[a,b], Changrong Zhou[b], Changlai Yuan[b], Wenhua Li[b], Minhong Jiang[b]

[a]School of Material Science and Engineering, Central South University, Changsha, Hunan 410083, PR China
[b]School of Material Science and Engineering, Guilin University of Electronic Technology, Guilin, Guangxi 541004, PR China

Received 13 August 2013; received in revised form 12 September 2013; accepted 2 October 2013
Available online 10 October 2013

Abstract

Lead-free $(1-x)(Ba_{0.85}Ca_{0.15})(Ti_{0.9}Zr_{0.1})O_3-xBiYbO_3$ $[(1-x)BCTZ-xBYO]$ piezoelectric ceramics in the range of BYO concentrations were prepared by the conventional oxide-mixed method, and the effect of BYO content on their microstructure, crystalline structure, density and electrical properties was investigated. A dense microstructure with large grain was obtained for the ceramics with the addition of BYO. The ceramics with $x=0.1\%$ exhibit an optimum electrical behavior of $d_{33}\sim580$ pC/N, $r\sim10.9\ \Omega$, $k_p\sim56.4\%$, and tan $\delta\sim1.12\%$ when sintered at a low temperature of $\sim1350\ ^\circ C$. When the measuring electric field is 40 kV/cm, the well-saturated and square-like *P–E* loops for the ceramics were observed with $P_r\sim12.2\ \mu C/cm^2$ and $E_c\sim1.83$ kV/cm.

Keywords: C. Piezoelectric properties; C. Ferroelectric properties; D. Perovskite; Microstructure

1. Introduction

Recently, due to environmental concerns, lead-free piezoceramics have been given to much attention [1–10]. In the search for lead-free piezoceramics candidates, such as $Bi_{0.5}Na_{0.5}TiO_3$ [5,6,11] and $K_{0.5}Na_{0.5}NbO_3$ [7,8,12] materials have been extensively conducted to improve their piezoelectric properties, but their piezoelectric constants are lower than that of lead zirconate titanate (PZT) piezoelectric ceramics [13–15]. Therefore, it is necessary to develop lead-free piezoceramics systems with higher piezoelectric properties to replace PZT ceramics.

In recent years, an increasing amount of research has been done on the new piezoelectric materials of the $BaTiO_3$-based ceramics systems [1–4,16–18]. In these systems, Mn- and Cu-modified $(1-x)BiFeO_3-xBaTiO_3$ ceramics exhibited a high T_c of $\sim485\ ^\circ C$, but with a low-field piezoelectric properties of $d_{33}\sim170$ pC/N, $k_p\sim34.2\%$, which was reported by Zhou [1]. In 2009, a surprisingly high piezoelectric property of $d_{33}\sim620$ pC/N has been reported for the $BaTiO_3$-based ceramics by Ren [18]. Since then, a new piezoelectric system $(Ba_{0.85}Ca_{0.15})(Ti_{0.9}Zr_{0.1})O_3$ (BCTZ) with a super high d_{33} was extensively investigated [16,19–21]. Hao et al. [22] showed that the samples with grain size $>10\ \mu m$ exhibit excellent piezoelectric properties as $d_{33}\sim470$ pC/N, $k_p\sim48\%$ using different sintering methods for BCTZ piezoceramics. Damjanovic et al. [17] reported that the temperature-induced anomalies in the dielectric, piezoelectric, elastic coefficients and Raman spectroscopy of BCTZ ceramics. The $[(Ba_{1-3x/2}Bi_x)_{0.85}Ca_{0.15}](Ti_{0.9}Zr_{0.1})O_3$ ceramics with $x=0.75\%$ exhibits an optimum electrical behavior of $d_{33}\sim361$ pC/N and $k_p\sim40.2\%$ [23]. In our previous study, CeO_2-modified BCTZ ceramics exhibited improved electrical properties of $d_{33}\sim600$ pC/N, $k_p\sim51\%$, tan $\delta\sim1.2\%$ [24]. In addition, Shi [25] found $(1-x)(0.36BiScO_3–0.64PbTiO_3)-xBiYbO_3$ piezoelectric ceramics to exhibit a good piezoelectric constant $d_{33}\sim443$ pC/N with a high Curie temperature of $T_c\sim450\ ^\circ C$. Feng et al. [26] stated that a very promising material of $xBiYbO_3–(1-x)PbTiO_3$ piezoelectric ceramics for a high Curie temperature (T_c up to 590 °C). And the BYO material has a high Curie temperature of $T_c\sim650\ ^\circ C$ [27].

*Corresponding author. Tel.: +86 731 88879343; fax: +86 731 88876692.
E-mail addresses: majiafengsir@163.com, majiafeng1295@126.com (J. Ma).

0272-8842/$ - see front matter
http://dx.doi.org/10.1016/j.ceramint.2013.10.010

In this present work, the microstructure, dielectric, piezoelectric, and ferroelectric properties of $(1-x)$BCTZ$-x$BYO ceramics were studied. With the optimized processing, the enhanced d_{33} and tan δ in the $(1-x)$BCTZ$-x$BYO system were obtained. These results show that the $(1-x)$BCTZ$-x$BYO ceramics with good electrical properties are induced by doping an optimum BYO content.

2. Experimental procedure

The $(1-x)(Ba_{0.85}Ca_{0.15})(Ti_{0.9}Zr_{0.1})O_3-xBiYbO_3$ [$(1-x)$ BCTZ$-x$BYO] (x=0, 0.05, 0.1, 0.2, 0.4, and 0.6%) ceramics were prepared by a conventional ceramics technique. The starting raw materials were TiO_2, Bi_2O_3, ZrO_2, Yb_2O_3, $BaCO_3$, and $CaCO_3$ (> 99.5%, Analytically pure). The powders in the stoichiometric ratio of the compositions were mixed thoroughly in ethanol using ZrO_2 balls for 20 h, and then dried and calcined at 1250 °C for 4 h in air. After the calcination, the mixture was wet ball-milled again for 10 h dried and granulated with 5 wt% PVA as a binder, and then pressed into green disks with diameters of 12 mm and thickness 1 mm under a pressure of 100 MPa. After burning off PVA at 600 °C for 2 h the disk samples were sintered at 1350 °C for 4 h in the sealed Al_2O_3 crucibles. Silver paste was screen-printed on the surfaces as electrodes and then fired at 600 °C for 40 min.

Phase purity and crystal structure were characterized using X-ray diffraction (XRD, Bruker D8-2-Advance, Bruker AXS, Germany). Volume density (ρ_v) and relative density (ρ_r) of the specimens were measured by the Archimedes method using deionized water as medium. Grain morphology of the samples was examined using scanning electron microscopy (SEM, JSM-5610LV/Noran-Vantage, JEOL, Tokyo, Japan). These ceramics were poled at 40 °C in a silicone oil bath under a dc field of 4 kV/mm for 20 min. The direct piezoelectric coefficient (d_{33}) was measured using a Berlincourt d_{33} meter (ZJ-3A, China) at 110 Hz. Piezoelectric and dielectric properties were measured using an impedance analyzer (Agilent 4294A, Agilent Technologies, America). The polarization–electric field (*P–E*) loops of ceramics were observed at different temperature and 1 Hz using a ferroelectric tester (Radiant Precision Work-station, America) with a programmable 9023 Delta Design oven (Delta Design, San Diego, CA).

3. Results and discussions

The XRD patterns of $(1-x)$BCTZ$-x$BYO ceramics are shown in Fig. 1a. These data show that all ceramics are consistent with a single phase perovskite and no secondary phases were detected [28]. This result indicates that a stable solid solution is formed between BCTZ and BYO in this work range of $0<x<0.6\%$. Fig. 1b shows the expanded XRD patterns in the 2θ range of 45–45.5° of $(1-x)$BCTZ$-x$BYO piezoelectric ceramics. At room temperature, there are different peak shapes for these ceramics with the increase of BYO content. The $(1-x)$BCTZ$-x$BYO ceramic exhibits a coexistence of tetragonal and rhombohedral phases with splitting of the (002) and (200) peaks [4,29]. As x increases, the $(1-x)$ BCTZ$-x$BYO ceramics have a feature with obvious splitting of the (002) and (200) peaks, and increase a intensity ratio of the tetragonal and rhombohedral (002)/(200). The $(1-x)$ BCTZ$-x$BYO ceramics with the increase of x to 0.1%, the integrated diffraction intensity of the (200) peak nearly increases to the value of the integrated diffraction intensity of the (002) peak, as shown in Fig. 1b. The morphotropic phase boundary (MPB) between rhombohedral and tetragonal is always obtained in this work range of $0<x<0.6\%$ [21,30].

Fig. 2 shows the effect of x on the Volume density (ρ_v) and relative density (ρ_r) of $(1-x)$BCTZ$-x$BYO ceramics sintered at 1350 °C for 4 h. With increasing BYO content, the ρ_v and ρ_r of the ceramics first increase evidently, reach their maximum value of $\rho_v \sim 5.612$ g/cm^3 and $\rho_r \sim 98.2\%$ at $x=0.1\%$ and then decrease slightly as $x>0.1\%$. Hence, we can see that a small amount of BYO content help to enhance the density of ceramics and lower the sintering temperature. The surface microstructure of $(1-x)$BCTZ$-x$BYO ceramics sintered at 1350 °C for 4 h are shown in Fig. 3. Grain size obviously was

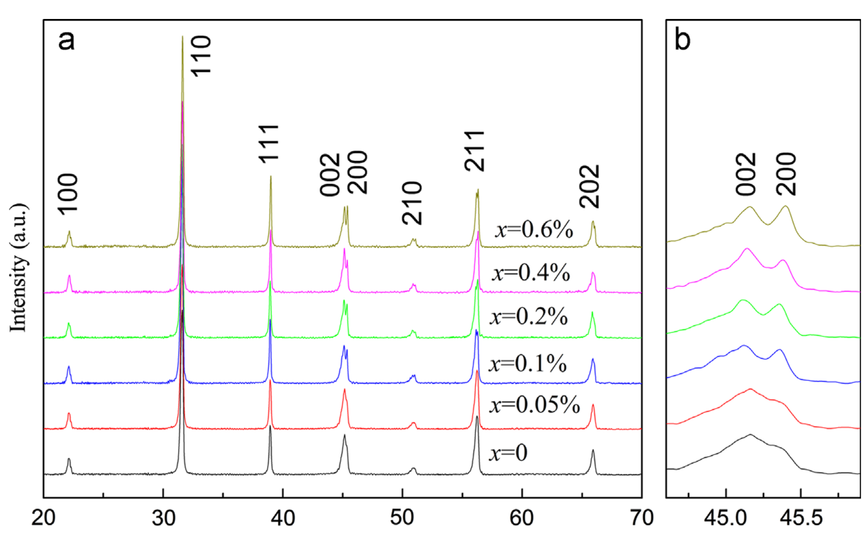

Fig. 1. (a) XRD patterns and (b) expanded XRD patterns of $(1-x)$BCTZ$-x$BYO ceramics as a function of x.

increased with the amount of BYO addition and the grain growth was inhibited with further increasing BYO content. When the $(1-x)$BCTZ$-x$BYO ceramics is at $x=0.05\%$, the grains became slightly larger and more uniform in Fig. 3b. With the increase of x to 0.1%, the ceramics are well possess a dense microstructure and distinct grains of diameter about 20–25 μm uniformly distributed among the grains in Fig. 3c. The ceramics have an unhomogeneous grain growth and large grains of >20 μm with small amount of small grains of 1–3 μm in boundary are observed as the introduction of further BYO content ($x>0.4\%$) gather into crystal boundary of the $(1-x)$BCTZ$-x$BYO ceramics in Fig. 3e and f. Grain size greatly affects the extrinsic contributions to the piezoelectric performance [31].

Fig. 4a plots the piezoelectric coefficient (d_{33}) and resonant resistance (r) values of $(1-x)$BCTZ$-x$BYO ceramics with different BYO content, measured at room temperature. The d_{33} value increases with small addition of BYO content, reaches the maximum value of $d_{33}\sim580$ pC/N at $x=0.1\%$, and then quickly decreases with a further increasing BYO content. Opposite, the r value firstly decreases, gets the minimum (~10.9 Ω) at $x=0.1\%$, and then slightly increases. The above results show that the larger d_{33} and smaller r values of BCTZ ceramics to meet the high-power piezoelectric devices [32]. In this work, the d_{33} value of $(1-x)$BCTZ$-x$BYO ceramics is much better than those reported of BCTZ ceramics [4,19,33]. Fig. 4b shows the electromechanical coupling factor (k_p) and mechanical quality factor (Q_m) of $(1-x)$BCTZ$-x$BYO ceramics as a function of x, measured at room temperature. The k_p value increases, reaches a maximum of $k_p\sim56.4\%$ for the ceramic with $x=0.1\%$, and then decreases with further increasing BYO content. The Q_m value of $(1-x)$BCTZ$-x$BYO ceramics exhibits a similar change of k_p's, obtains the maximum ($Q_m\sim152.7$) for the ceramic with $x=0.05\%$. The k_p value of BCTZ ceramics in this work is better than those of BCTZ ceramics [22,24,28,31,34]. Therefore, ferroelectric properties of $(1-x)$BCTZ$-x$BYO ceramics were enhanced with small amount of BYO content because of the microstructure of $(1-x)$BCTZ$-x$BYO ceramics is much denser than the pure BCTZ ceramics, as shown in Figs. 2 and 3.

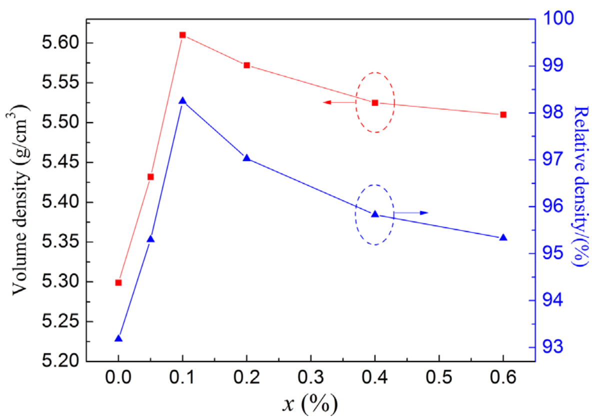

Fig. 2. Volume density and relative density of $(1-x)$BCTZ$-x$BYO ceramics as a function of x.

Fig. 5a reveals the dielectric constant (ε_r) and dielectric loss (tan δ) for the $(1-x)$BCTZ$-x$BYO samples as a function of BYO content at room temperature. With the increase of BYO content, the ε_r of the ceramics first increases evidently, reaches its maximum value of $\varepsilon_r\sim4714$ at $x=0.1\%$ and then decreases slightly. Opposite, by adding small amounts of BYO to BCTZ ceramics, the tan δ value first decreases evidently and then increases again, obtains a minimum of tan $\delta\sim1.12\%$ for the ceramics with $x=0.1\%$. These results further indicate that the lower value of tan δ is due to the denser microstructure. Fig. 5b reveals temperature dependence of dielectric constant ε_r at 1 kHz for the $(1-x)$BCTZ$-x$BYO ceramics sintering at 1350 °C for 4 h. It can be seen that there are two peaks for the $(1-x)$BCTZ$-x$BYO ceramics as a function of BYO content in the measured temperature range from –30 to 130 °C. when doping small amounts of BYO content ($x\le0.1\%$), the Curie temperature T_c and the temperature of rhombohedral-tetragonal phase transition T_{R-T} peaks all shift slightly low temperature. While increasing the BYO content, the T_c and T_{R-T} peaks all shift to low temperature and the (ε_m)

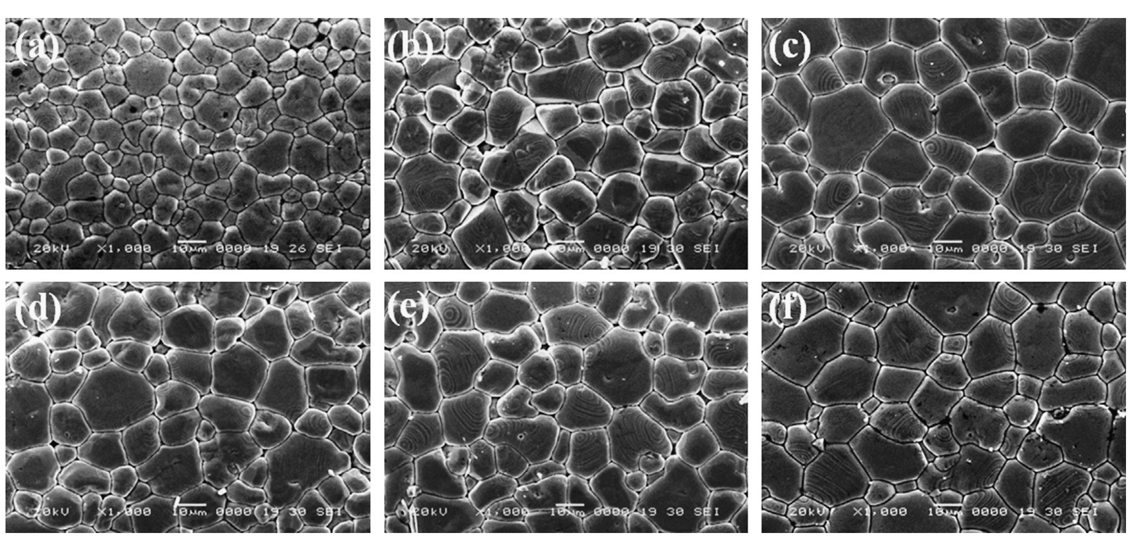

Fig. 3. SEM micrographs of $(1-x)$BCTZ$-x$BYO ceramics with (a) $x=0$, (b) $x=0.05\%$, (c) $x=0.1\%$, (d) $x=0.2\%$, (e) $x=0.4\%$, and (f) $x=0.6\%$.

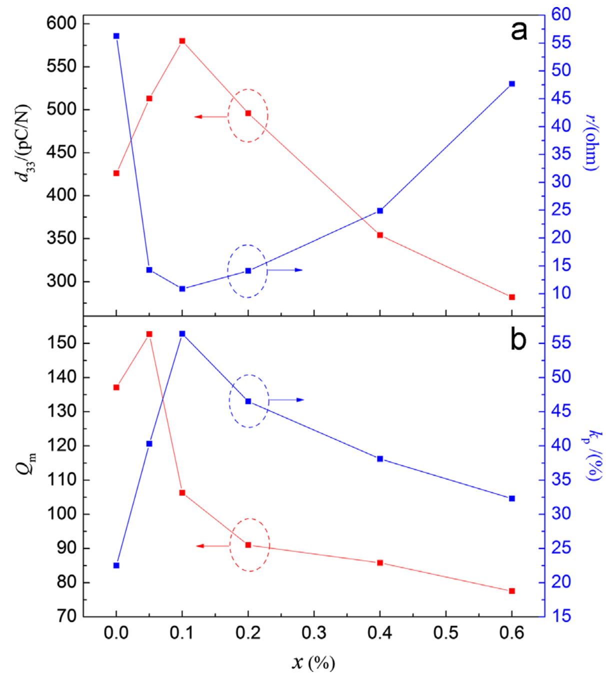

Fig. 4. Piezoelectric properties of $(1-x)$BCTZ$-x$BYO ceramics as a function of x, (a) d_{33} and r, (b) k_p and Q_m.

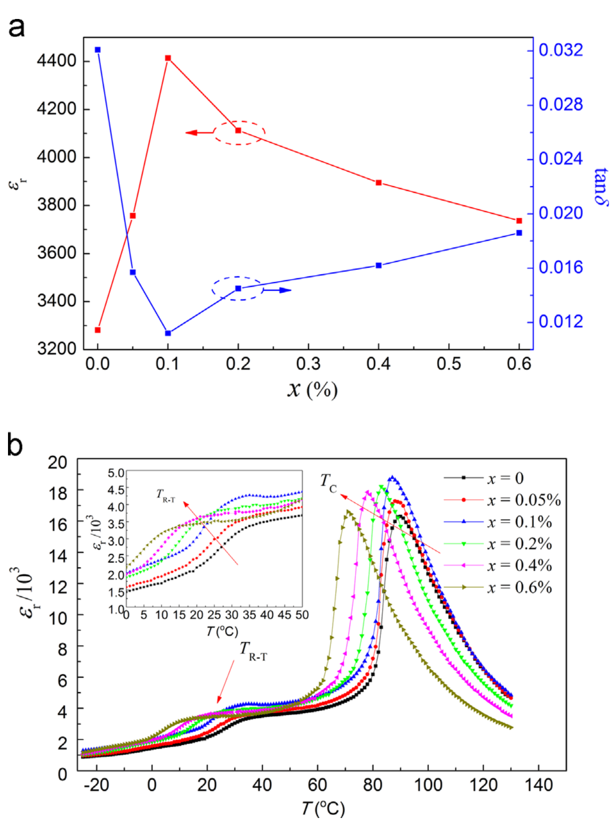

Fig. 5. (a) Dielectric properties and (b) temperature dependence of the ε_r and tan δ of $(1-x)$BCTZ$-x$BYO ceramics as a function of x at 1 kHz.

values (ε_r value at T_c) were increased slightly for the $(1-x)$ BCTZ$-x$BYO ceramics. It can be noted with the fact that BYO doping does not improve the Curie temperature of $(1-x)$ BCTZ$-x$BYO ceramics, which is contrary to our expectation. However, as is well known, the BYO material has a high Curie temperature of $T_c \sim 650$ °C [27].

Fig. 6a shows the P–E curves of $(1-x)$BCTZ$-x$BYO ceramics with different BYO contents, measured under the electric field of 4 kV/mm and at room temperature. All samples exhibit well typical P–E hysteresis loops when measured at the frequency of 1 Hz. While increasing the BYO content, the remnant polarization P_r first increased, reaches a maximum value of 12.2 μC/cm^2 at $x=0.1\%$, and then reduced rapidly with further increasing of x. On the other hand, the coercive field E_c decreases significantly with the increase of x. For $x=0.1\%$ sample, E_c acquires a minimum value of 1.83 kV/cm. Fig. 6b plots the polarization versus electric field of the $(1-x)$ BCTZ$-x$BYO ceramics with $x=0.1\%$ and under the electric field of 4 kV/mm measured at different temperatures. P_r decreases from 15.4 to 1.1 μC/cm^2 as the measured temperature increases from −60 to 100 °C. The values of the P_r presents uniformity variations (~1 μC/cm^2 every 20° in the

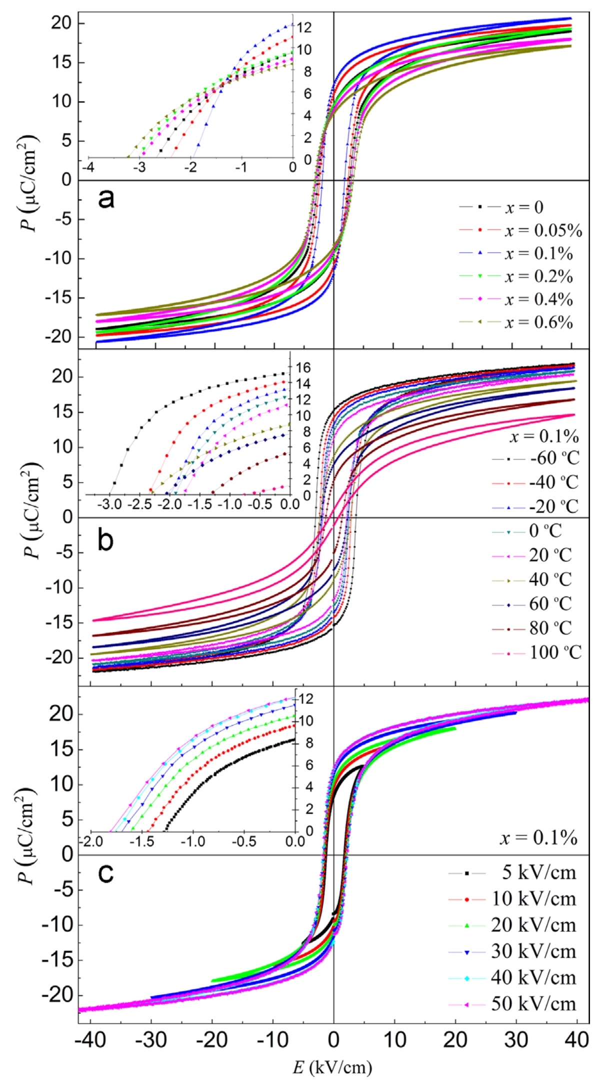

Fig. 6. (a) P–E loops of $(1-x)$BCTZ$-x$BYO ceramics as a function of x, (b) temperature dependence of P–E loops of $(1-x)$BCTZ$-x$BYO ceramics at $x=0.1\%$ measured from −60 to 100 °C, and (c) the room temperature P–E loops of $(1-x)$BCTZ$-x$BYO ceramics at $x=0.1\%$ measured at different fields.

range −60 to 20 °C) from 15.4 to 11.5 μC/cm^2. And then, the *P–E* hysteresis loops become slimmer while increasing the temperature, accompanied by a fast drop of P_r values. Last, the *P–E* curves looks almost closed at the temperature of ~100 °C, indicating that ferroelectric domains disappear. However, the E_c value of the $(1-x)$BCTZ$-x$BYO ceramics with $x=0.1\%$ gradually decreases with the increase of the temperature from −60 to 20 °C, and then dramatically increases from 1.76 to 3.1 kV/cm as the measured temperature in the range 20 to 40 °C, finally, decreases from 3.1 to 0 kV/cm with further increasing of the temperature from 40 to 100 °C, also owing to the involvement of the rhombohedral-tetragonal phase transition. These results are in good agreement with that of T_{R-T}'s as shown in Fig. 5b. Fig. 6c shows the room temperature *P–E* hysteresis loops of the $(1-x)$BCTZ$-x$BYO ceramics with $x=0.1\%$ measured at different fields. Because of the high coercive field E_c, the ceramics exhibits a low *P–E* loop under an electric field of 5–30 kV/cm, giving a small value of remnant polarization P_r. With the measuring electric field increase to 40 kV/cm, the well-saturated and square-like *P–E* loops for the ceramics were observed, P_r reaches a maximum value of 12.2 μC/cm^2 and E_c acquires a value of 1.83 kV/cm. As shown in Fig. 6a, b, and c, the addition of small amount of BYO with $x=0.1\%$ measured at 40 kV/cm was quite effective to improve P_r from 9.3 to 12.2 μC/cm^2 and decrease E_c from 2.82 to 1.83 kV/cm.

4. Conclusions

Lead-free $(1-x)$BCTZ$-x$BYO ceramics were prepared by the conventional solid-state method when sintered at a low temperature of 1350 °C for 4 h. The XRD patterns show that the addition of BYO did not change the crystal structure of all ceramics and all ceramics are consistent with a single phase perovskite. The average grain size and relative density of the ceramics obviously increases bigger with the addition of BYO, a dense microstructure with large grain was obtained for the ceramics. The Curie temperature decreases with increasing the BYO content. The decrease in dielectric loss should be chiefly attributed to the dense microstructure caused by BYO. An enhanced electrical behavior of d_{33}~580 pC/N, k_p~56.4%, ε_r~4714, P_r~12.2 μC/cm^2, and E_c~1.83 kV/cm is demonstrated for the ceramic with $x=0.1\%$.

Acknowledgments

This work was supported by the National Nature Science Foundation of China (NSFC nos. 61261012, 51102055, 51102056, and 51201043) and Guangxi Science Foundation (2010GXNSFD013007).

References

[1] Changrong Zhou, Antonia Feteira, Xu Shan, Huabin Yang, Qin Zhou, Jun Cheng, Weizhou Li, Hua Wang, Remarkably high-temperature stable piezoelectric properties of $Bi(Mg_{0.5}Ti_{0.5})O_3$ modified $BiFeO_3-BaTiO_3$ ceramics, Applied Physics Letters 101 (2012) 032901-0–032901-4.

[2] Sandeep Mahajan, Divya Haridas, K. Sreenivas, O.P. Thakur, Chandra Prakash, Enhancement in electro-strain behavior by La^{3+} substitution in lead free $BaZr_{0.05}Ti_{0.95}O_3$ ceramics, Materials Letters 97 (2013) 40–43.

[3] Zhengyong Cen, Changrong Zhou, Jun Cheng, Xiujuan Zhou, Li Weizhou, Chunle Yan, Songlin Feng, Yueqiang Liu, Daosong Lao, Effect of Zr^{4+} substitution on thermal stability and electrical properties of high temperature $BiFe_{0.99}Al_{0.01}O_3$-$BaTi_{1-x}Zr_xO_3$ ceramics, Journal of Alloys and Compounds 567 (2013) 110–114.

[4] Jiagang Wu, Dingquan Xiao, Wenjuan Wu, Qiang Chen, Jianguo Zhu, Zhengchun Yang, John Wang, Composition and poling condition-induced electrical behavior of $(Ba_{0.85}Ca_{0.15})(Ti_{1-x}Zr_x)O_3$ lead-free piezoelectric ceramics, Journal of the European Ceramic Society 32 (2012) 891–898.

[5] Werner Krauss, Denis Schütz, Franz Andreas Mautner, Antonio Feteira, Klaus Reichmann, Piezoelectric properties and phase transition temperatures of the solid solution of $(1-x)(Bi_{0.5}Na_{0.5})TiO_3-xSrTiO_3$, Journal of the European Ceramic Society 30 (2010) 1827–1832.

[6] Jianjun Yao, Niven Monsegue, Mitsuhiro Murayama, Weinan Leng, William T. Reynolds, Qinhui Zhang, Haosu Luo, Jiefang Li, Wenwei Ge, D. Viehland, Role of coexisting tetragonal regions in the rhombohedral phase of $Na_{0.5}Bi_{0.5}TiO_{3-}x$ at.% $BaTiO_3$ crystals on enhangced piezoelectric properties on approaching the morphotropic phase boundary, Applied Physics Letters 100 (2012) 012901-0–012901-4.

[7] X. Vendrell, J.E. García, F. Rubio-Marcos, D.A. Ochoa, L. Mestres, J.F. Fernández, Exploring different sintering atmospheres to reduce nonlinear response of modified KNN piezoceramics, Journal of the European Ceramic Society 33 (2013) 825–831.

[8] J. Taub, L. Ramajo, M.S. Castro, Phase structure and piezoelectric properties of Ca- and Ba-doped $K_{1/2}Na_{1/2}NbO_3$ lead-free ceramics, Ceramics International 39 (2013) 3555–3561.

[9] Chun-Ming Wang, Shujun Zhang, Jin-Feng Wang, Ming-Lei Zhao, Chun-Lei Wang, Electromechanical properties of calcium bismuth niobate ($CaBi_2Nb_2O_9$) ceramics at elevated temperature, Materials Chemistry and Physics 118 (2009) 21–24.

[10] S.-B. Lee, T.S. Key, Z. Liang, R.E. García, S. Wang, X. Tricoche, G.S. Rohrer, Y. Saito, C. Ito, T. Tani, Microstructure design of lead-free piezoelectric ceramics, Journal of the European Ceramic Society 33 (2013) 313–326.

[11] Ke Wang, Ali Hussain, Wook Jo, Jürgen Rödel, Temperature-dependent properties of $(Bi_{1/2}Na_{1/2})TiO_3$-$(Bi_{1/2}K_{1/2})TiO_3$–$SrTiO_3$ lead-free piezoceramics, Journal of the American Ceramic Society 95 (2012) 2241–2247.

[12] Huabin Yang, Changrong Zhou, Qin Zhou, Changlai Yuan, Weizhou Li, Hua Wang, Lead-free (Li, Na, K)(Nb, Sb)O_3 modification and sintering temperature on microstructure and electrical properties, Journal of Materials Science 48 (2013) 2997–3002.

[13] Liaodong Ai, Xiuzhi Li, Zujian Wang, Ying Liu, Chao He, Tao Li, Tao Chu, Dongfang Pang, Hamel Tailor, Xifa Long, Preparation, structure, and electric properties of the $Pb(Zn_{1/3}Nb_{2/3})O_3$-$Pb(Yb_{1/2}Nb_{1/2})O_3$-$PbTiO_3$ ternary ferroelectric system ceramics near the morphotropic phase boundary, Journal of the European Ceramic Society 33 (2013) 2155–2165.

[14] Huajun Kang, Jun Chen, Laijun Liu, Liang Fang, Xianran Xing, Temperature dependences of the ferroelectric and dielectric properties of high curie temperature $PbTiO_3$-$BiScO_3$-$Bi(Zn_{1/2}Zr_{1/2})O_3$, Materials Research Bulletin 48 (2013) 2006–2009.

[15] Mupeng Zheng, Yudong Hou, Haiyan Ge, Mankang Zhu, Hui Yan, The formation of (Zn, Ni)TiO_3 secondary phase in NiO-modified $Pb(Zn_{1/3}Nb_{2/3})O_3$-$PbZrO_3$-$PbTiO_3$ ceramics, Scripra Materialia 68 (2013) 707–710.

[16] Jiagang Wu, Xiao Dingquan, Wu Wenjuan, Jianguo Zhu, John Wang, Effect of dwell time during sintering on piezoelectric properties of $(Ba_{0.85}Ca_{0.15})(Ti_{0.9}Zr_{0.1})O_3$ lead-free ceramics, Journal of Alloys and Compounds 509 (2011) L359–L361.

[17] Dragan Damjanovic, Alberto Biancoli, Leili Batooli, Amirhossein Vahabzadeh, Joe Trodahl, Elastic, dielectric, and piezoelectric anomalies and raman spectroscopy of $0.5Ba(Ti_{0.8}Zr_{0.2})O_3$-$0.5(Ba_{0.7}Ca_{0.3})TiO_3$, Applied Physics Letters 100 (2012) 192907-0–192907-4.

[18] Wenfeng Liu, Xiaobing Ren, Large piezoelectric effect in Pb-free ceramics, Physical Review letters 103 (2009) 257602-0–257602-4.

[19] Chao Han, Jiagang Wu, Chaohui Pu, Sha Qiao, Bo Wu, Jianguo Zhu, Dingquan Xiao, High piezoelectric coefficient of Pr_2O_3-doped $(Ba_{0.85}Ca_{0.15})(Ti_{0.9}Zr_{0.1})O_3$ ceramics, Ceramics International 38 (2012) 6359–6363.

[20] S.K. Ye, J.Y.H. Fuh, L. Lu, Structure and electrical properties of ⟨001⟩ textured $(Ba_{0.85}Ca_{0.15})(Ti_{0.9}Zr_{0.1})O_3$ lead-free piezoelectric ceramics, Applied Physics Letters 100 (2012) 252906-0–252906-4.

[21] Ye Tian, Lingling Wei, Xiaolian Chao, Zonghuai Liu, Zupei Yang, Phase transition Behavior and Large Piezoelectricity near the morphotropic phase boundary of lead-free $(Ba_{0.85}Ca_{0.15})(Ti_{0.9}Zr_{0.1})O_3$ ceramics, Journal of the American Ceramic Society 96 (2013) 496–502.

[22] Jigong Hao, Wangfeng Bai, Wei Li, Jiwei Zhai, Correlation between the microstructure and electrical properties in high-performance $(Ba_{0.85}Ca_{0.15})(Ti_{0.9}Zr_{0.1})O_3$ lead-free piezoelectric ceramics, Journal of the American Ceramic Society 95 (2012) 1998–2006.

[23] Tao Chen, Ting Zhang, Jifang Zhou, Jianwei Zhang, Yuhong Liu, Guangchang Wang, Ferroelectric and piezoelectric properties of $[(Ba_{1-3x/2}Bi_x)_{0.85}Ca_{0.15}](Ti_{0.9}Zr_{0.1})O_3$ lead-free piezoelectric ceramics, Materials Research Bulletin 47 (2012) 1104–1106.

[24] Yerang Cui, Xinyu Liu, Minhong Jiang, Xiayan Zhao, Xu Shan, Wenhua Li, Changlai Yuan, Changrong Zhou, Lead-free $(Ba_{0.85}Ca_{0.15})(Ti_{0.9}Zr_{0.1})O_3$-$CeO_2$ ceramics with high piezoelectric coefficient obtained by low-temperature sintering, Ceramics International 38 (2012) 4761–4764.

[25] Wei Shi, Ying Pei, Jianshuai Wei, Qiang Chen, Dingquan Xiao, Jiangguo Zhu, Dielectric and piezoelectric Properties of $(1-x)(0.36BiScO_3$-$0.64PbTiO_3)-xBiYbO_3$ ceramics, Ferroelectrics 409 (2010) 3–7.

[26] Gao Feng, Hong Rongzi, Liu Jiaji, Li Zhen, Cheng Lihong, Tian Chang Sheng, Phase formation and characterization of high Curie temperature $xBiYbO_3$-$(1-x)PbTiO_3$ piezoelectric ceramics, Journal of the European Ceramics Society 29 (2009) 1687–1693.

[27] Richard E. Eitel, Clive A. Randall, Thomas R. Shrout, Paul W. Rehrig, Wes Hackenberger, Seung-Eek Park, New high temperature morphotropic phase boundary piezoelectrics based on $Bi(Me)O_3$-$PbTiO_3$ ceramics, Japanese Journal of Applied Physics 40 (2001) 5999–6002.

[28] Jiagang Wu, Wenjuan Wu, Dingquan Xiao, John Wang, Zhenchun Yang, Zhihang Peng, Qiang Chen, Jianguo Zhu, (Ba, Ca)(Ti, Zr)O_3-$BiFeO_3$ lead-free piezoelectric ceramics, Current Applied Physics 12 (2011) 534–538.

[29] Tao Chen, Ting Zhang, Guangchang Wang, Jifang Zhou, Jianwei Zhang, Yuhong Liu, Effect of CuO on the microstructure and electrical properties of $Ba_{0.85}Ca_{0.15}Ti_{0.90}Zr_{0.10}O_3$ piezoceramics, Journal of Materials Science 47 (2012) 4612–4619.

[30] Yuqing Lei, Hong Wu, Dunmin Lin, Qiaoji Zheng, Xiaochun Wu, Ximing Fan, Phase transition, dielectric and piezoelectric properties of $NaNbO_3$-$Ba_{0.85}Ca_{0.15}(Ti_{0.9}Zr_{0.1})O_3$ lead-free ceramics, Functional Materials Letters 5 (2012) 1250033–1250033-4.

[31] Qin Zhou, Changrong Zhou, Huabin Yang, Guohua Chen, Weizhou Li, Hua Wang, Dielectric, ferroelectric, and piezoelectric properties of $Bi(Ni_{1/2}Ti_{1/2})O_3$-modified $BiFeO_3$-$BaTiO_3$ ceramics with high Curie temperature, Journal of the American Ceramic Society 95 (2012) 3889–3893.

[32] Yongkang Gao, Yun-Han Chen, Jungho Ryu, Kenji Uchino, Dwight Viehland, Eu and Yb substituent effects on the properties of $Pb(Zr_{0.52}Ti_{0.48})O_3$–$Pb(Mn_{1/3}Sb_{2/3})O_3$ ceramics: development of a new high-power piezoelectric with enhanced vibrational velocity, Japanese Journal of Applied Physics 40 (2001) 687–693.

[33] Jiagang Wu, Dingquan Xiao, Bo Wu, Wenjuan Wu, Jianguo Zhu, Zhengchun Yang, John Wang, Sintering temperature-induced electrical properties of $(Ba_{0.9}Ca_{0.1})(Ti_{0.85}Zr_{0.1})O_3$ lead-free ceramics, Materials Research Bulletin 47 (2012) 1281–1284.

[34] Pan Wang, Yongxiang Li, Yiqing Lu, Enhanced piezoelectric properties of $(Ba_{0.85}Ca_{0.15})(Ti_{0.90}Zr_{0.10})O_3$ lead-free ceramics by optimizing calcinations and sintering temperature, Journal of the European Ceramics Society 31 (2011) 2005–2012.